J. Biomed. Eng. Res.
Vol. 20, No. 2, 173-181, 1999

Pharmacokinetic Compartment Modeling을 이용한 나선식 CT에서의 간암-간 대조 곡선의 Simulation

김수정·이경호*·한준구*·김종효*·민병구**

서울대학교 대학원 협동과정 의용생체공학 전공, *의과대학 방사선과학 교실, **의과대학 의공학 교실
(1998년 10월 19일 접수, 1999년 3월 4일 채택)

Simulation of lesion-to-liver contrast difference curves in Dynamic Hepatic CT with Pharmacokinetic Compartment Modeling

S.J. Kim, K.H. Lee*, J.H. Kim*, J.K. Han*, B.G. Min**

Department of Biomedical Engineering, College of Engineering, Seoul National University
*Department of Radiology, College of Medicine, Seoul National University
**Department of Biomedical Engineering, College of Medicine, Seoul National University
(Received October 19, 1998, Accepted March 4, 1999)

요 약 : 조영 증강제를 이용한 나선식 CT는 간 질환을 진단하는데 있어 중요한 역할을 하고있음에도 불구하고 진단의 효율을 최적화하는 프로토콜은 명확하게 알려져 있지 않다. 따라서 나선식 CT에서의 간암-간 대조 곡선을 모의 실험(simulation) 하여 다양한 요소들이 시간-조영 곡선에 어떻게 영향을 미치는지 파악하고, 또한 CT 검사 전에 모의 실험을 하여 이론적으로 최적의 스캔을 할 수 있도록 하기 위하여 약동학(pharmacokinetics)에 기초한 compartment model을 구성하였다. 간암, 간, 대동맥 및 간문맥 등을 각 구획(compartment)으로 설정하여 각 구획에서의 미분방정식을 얻은 후 적분하여 Hounsfield unit 값을 조영제 주입 후 시간의 함수로 얻었으며 각 구획의 시간-조영 곡선을 출력하였다. 구현한 프로그램에서는 간암의 크기 및 종양 혈관의 분포 등과 같은 간암의 성질, 간경화의 정도에 따른 간 혈관 공급의 양상 및 조영제의 부피, 농도, 주입 속도 등의 조영제 주입 방법, 환자의 몸무게, 키 등의 환자의 신체 계수, 그리고 심박출량 등의 환자의 혈역학적 계수 등을 입력 받아 간암을 비롯한 각 구획의 시간-조영 곡선 및 간-간암 대조 곡선을 출력할 수 있도록 하였다. 모델링을 통해 얻은 조영 증강 곡선은 같은 환경하에서 얻은 24명의 환자 데이터와 비교하여 유사한 결과를 얻을 수 있었으며, 조영 증강제 주입 방법의 변화가 간암-간 대조 곡선에 미치는 영향을 비교할 수 있었다.

Abstract : Contrast-enhanced CT has an important role in assessing liver lesions. However, the optimal protocol to get most effective result is not clear. The main goal when deciding injection protocol is to optimize lesion detectability with rapid scanning when lesion to liver contrast is maximum. For this purpose, we developed a physiological model of the contrast medium enhancement based on the compartment modeling and pharmacokinetics. Blood supply to liver is achieved in two paths. This dual supply characteristic distinguishes the CT enhancement of liver from that of the other organs. The first path is by hepatic artery and the second, by portal vein. However, it is assumed that only hepatic artery can supply blood to hepatocellular carcinoma(HCC) compartment, thus, the difference of contrast enhancement is resulted between normal liver tissue and hepatic tumor. By solving differential equations for each compartment simultaneously using the computer program Matlab, CT contrast-enhancement curves were simulated. The simulated enhancement curves for aortic, hepatic, portal vein, and HCC compartments were compared with the mean enhancement curves from 24 patients exposed to the same protocols as the simulation. These enhancement curves showed a good agreement. Furthermore, we simulated lesion-to-liver curves for various injection protocols, and the effects were analyzed. The variables to be considered in the injection protocol were injection rate, dose, and concentration of contrast material. These data may help to optimize scanning protocols for better diagnosis.
Key words : contrast-enhanced CT, optimal protocol, lesion to liver contrast, pharmacokinetics, compartment modeling, simulation

통신저자 : 김수정, (110-744) 서울 종로구 연건동 28 서울대학병원 임상의학연구소 5301호,
Tel. (02)760-1762, Fax. (02)747-3200

INTRODUCTION

Many abdominal CT applications necessitate intravenous administration of contrast medium to enhance lesion conspicuity. However, the optimal technique for injection is not clear. The main principle for deciding injection protocol is to optimize lesion detectability by rapid scanning when lesion to liver contrast is maximum, because lesion detection is identifying differences in appearance between what is considered normal and abnormal[1]. Therefore we should find the protocol not only to maximize contrast difference between normal and abnormal tissue resulting from a nonequal distribution of contrast media but also to elongate the time period during which the lesion detection is clear.

To determine the injection protocol and timing of the initiation and completion of dynamic CT scanning, it is very useful to understand pharmacokinetics of contrast medium. Contrast media enhanced tumor identification can be performed either according to the vascularization of the lesion, or by using the permeability of the endothelium and the accessible extravascular space[2]. Because of the extracellular distribution of contrast media, rapid extravasation occurs and compounds leave the vascular compartment within seconds after injection and equilibrate in the total extracellular space[2]. The separate characterization of intravascular space and tissue parenchyma is possible only to a very limited extent because of the rapid extravasation process. In case the tumor is hypervascular, the chance to detect the lesion become high if imaging is performed during vascular phase. On the other hand, diffusion of contrast material into the extravascular space is a slower process in hypovascular metastases than in normal hepatic parenchyma[3]. That is, metastatic liver nodules of colorectal carcinoma are usually hypodense on contrast CT images so that maximum detectability may be attained at the peak enhancement of the liver[4]. Therefore, it will be useful to find the time period in which the difference of lesion enhancement from the hepatic enhancement is apparent in each case.

To investigate the effect of injection parameters of contrast medium on enhancement at computed tomography, we developed a pharmacokinetic model and simulated the resulted contrast enhancement.

We simulate the effect of various injection protocols using this model, and compare it with experimental and clinical data. By help of this simulation, one can choose optimal injection protocol. Furthermore, one can choose a scanning initiation time such that the first and last CT sections will have nearly equal enhancement of contrast[5] by using time- attenuation curve for that particular injection protocol, knowing how many sections will be imaged over what time interval in a dynamic series.

MATERIAL AND METHOD

1. Dual supply model for hepatic CT enhancement

We referred to[6] for simplified human cardiovascular system that consists of the heart, vascular networks, and key organs, and referred to[7] for the distributions of blood volume and flow throughout the body. The average blood volume for a typical adult was set to 5 L(3 L of plasma and 2 L of red blood cells) and the average cardiac output to be 6.5 L/min[6].

We assume each compartment as perfect mixing compartment, in which the mixing of the entering blood(and the substance it carries) with the original contents of the compartment is instantaneous and complete[8]. Intravenously administrated contrast medium(through an antecubital vein) is mixed in the right side of the heart and distributed through the vascular compartment and it is diffused rapidly to the extracellular compartment. Because CT contrast medium does not penetrate cells in general, the intracellular part of liver remains essentially free of contrast medium. Therefore we can neglect the intracellular compartment in the model. Contrast medium is eliminated by urine at a constant rate[9].

In the blood vessel compartments, regardless of the numbers of inlet and outlet, the input(qi) and output volumetric flow rates(qo) of the blood are assumed to be same, since we treat the constant volume of compartments($dV/dt=0$). The governing equation for this blood vessel compartment can be derived from mass conservation of contrast material, that is

$$V\frac{dC}{dt} = \Sigma q_{in} \cdot C_{in} - \Sigma q_{out} \cdot C \,, \qquad (1)$$

where C is the concentration of the contrast material of the compartment and Cin is that of the former compartment. In the model of organs, we must add one additional compartment representing the extracellular space of the organ to the capillary vessel compartment. In the capillary vessel

compartments, contrast materials are exchanged by two mechanisms. One is by volumetric blood flow like equation (1), and the other is by diffusion through capillary membranes that permits the exchange of materials among the capillary and extracellular space. Therefore the governing equation for the capillary compartment is,

$$V\frac{dC}{dt} = \Sigma q_{in} \cdot C_{in} - \Sigma q_{out} \cdot C - p \cdot s \cdot (C - C_{ec}) , \quad (2)$$

where C_{ec} is the concentration of extracellular compartment, p is permiability of vessel membrane, and s is diffusion surface area. And the following equation is for the extracellular compartment of lesion, where Vec is the volume of extracellular compartment.

$$V_{ec}\frac{dC_{ec}}{dt} = p \cdot s \cdot (C - C_{ec}). \quad (3)$$

The differential equations for each compartment were solved simultaneously. That is, we can get the contrast medium concentration in each compartment by integrating differential equations for each compartment simultaneously with respect to time. The model was implemented in PC using Runge-Kutta algorithm. We referred the result of Bae[9] for the relationship between CT enhancement and concentration.

Figure 1 shows a compartment model to illustrate the transport process of contrast medium to liver. For simplicity, only the compartments having direct relations with the blood supply to liver is designated. Blood is supplied to liver by two paths. This dual supply character distinguishes the CT enhancement of liver from that of the other organs. The first path is by hepatic artery and the second is by portal vein. In case hepatic lesion exists, it is regarded as independent compartment characterized by its vascularity and volume. We defined the vascularity as the parameter which designates how much the vascular volume in the lesion exceeds normal value. It considers not only vascular volume in tumor, but also the permeability and diffusion surface different from normal value. These values are made variable in the simulation program according to the type of lesion. It is assumed that only hepatic artery can supply blood to this compartment. It is known that this causes the difference of contrast enhancement between normal liver tissue and hepatic tumor. At two phase contrast-enhanced helical CT to detect and characterize hepatocellular carcinoma (HCC), the typical enhancement pattern of HCC is hyperattenuating compared with the hepatic parenchyma during the early phase and hypoatteneuating during the delayed phase. The differential equations for HCC compartment can be written as follows.

$$V_{hcc}\frac{dC_{hcc}}{dt} = q_{ha} \cdot C_{ha} - q_{hcc} \cdot C_{hcc} - p \cdot s \cdot (C_{hcc} - C_{ec}) \quad (4)$$

$$V_{ec}\frac{dC_{ec}}{dt} = p \cdot s \cdot (C_{hcc} - C_{ec}) \quad (5)$$

Where V_{hcc}, C_{hcc} are volume and contrast medium concentration of HCC capillary compartment respectively, and q_{ha} is the volume flow rate from hepatic artery to HCC compartment.

Simulations were performed for the physiological parameters of typical adults. These parameters can be varied, if we know the total blood volume and cardiac output for the indivisual patient. According to the sex, weight(w in pounds), and height(h in inches) of given patient, the blood volume is calculated by $33.164 \times h^{0.725} \times w^{0.425} - 1{,}229$ for a man, and by $34.85 \times h^{0.725} \times w^{0.425} - 1{,}954$ for a woman. The equation for cardiac output is $36.36 \times h^{0.725} \times w^{0.425}$ both for a woman and a man[6]. We varified this model by comparing the simulation results with both the clinical data obtained from 24 patients who were refered for the trans arterial hemoembolization of HCC. And then, we tried to find the optimal injection protocol, and scanning time to coinside with the phase of maximal timor conspicuity. The visualization of hepatic tumors at CT was expressed by lesion conspicuity that is the attenuation of tumor subtracted by attenuation of hepatic parenchyma.

2. Acquisition of experimental and clinical data

All scans were obtained with helical CT scanner(HiSpeed Advantage; General Electric Medical System, Milwaukee, Wis) with use of 210 mA, 120 kVp, and beam collimation of 10 mm. In the study of 24 patients who have transarterial chemoembolization of HCC, the noncontrast incremental CT scans for the liver were acquired to determine the representative anatomic level with the tumor. The determined single anatomic level was scanned dynamically after injecting 150 ml of contrast material, corresponding to an iodine load of 45 g at a rate of 3 ml/sec using power injector. The single-level dynamic scan was composed of three phases. Each phase lasted for 31 seconds with breath hold. Sixteen scans were acquired every two seconds during

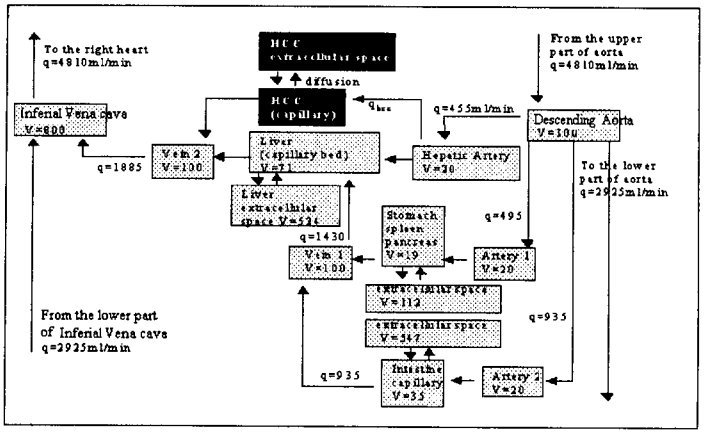

Fig. 1. Compartment model to illustrate the transport process of contrast medium to liver. Blood is supplied to liver by both hepatic artery(HA) and portal vein. On the other hand, it is assumed that only hepatic artery can supply blood to HCC compartment. This causes the difference of contrast enhancement between normal liver tissue and hepatic tumor

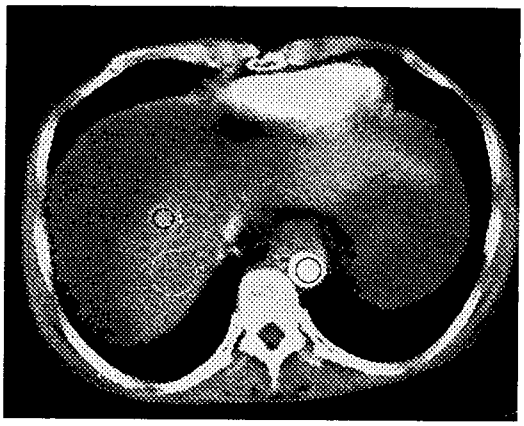

Fig. 2. ROI selection to obtain CT number-time curve in liver Dynamic Scan Image. Using region of interest (ROI) cursors at the CT console, mean attenuation values for the tumor, hepatic parenchyma, aorta, and portal vein on each image of single-level bolus dynamic CT were recorded. ROI 1: Hepatoma, ROI 2: Hepatic parenchyma, ROI 3: Aorta

first phase and 11 scans were acquired every three seconds during second and third phases. There were interphase delays between the scanning phases for patient breathing. The attenuation values for every second time point between the actual data points were estimated with linear interpolation. The attenuation values for every second time point during the interphase delays were estimated in the same manner. Using circular region of interest (ROI) cursors at the CT console, we recorded mean attenuation values for the tumor, hepatic parenchyma, aorta, and portal vein on each image of single-level bolus dynamic CT [figure 2]. And then, the attenuation difference between the tumor and hepatic parenchyma was calculated to find the region of best conspicuity.

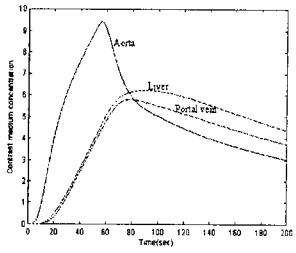

Fig. 3. A simulated example for contrast medium concentration in aorta, liver parenchyma, and portal vein after injection of 150 ml of contrast medium with the concentration of 300 mg/ml. The injection rate was set to 3 ml/sec

RESULTS

1. Simulation and Analysis

Contrast medium concentration as a function of time was obtained by solving all the governing equations simultaneously. We integrated differential equations for each compartment simultaneously with respect to time using Runge-Kutta method. Figure 4 shows a simulated example for contrast medium concentration in aorta and liver parenchyma after injection of 150 ml of contrast medium with the concentration of 300mg/ml. The injection rate was set to 3 ml/sec. There is a time delay in concentration enhancement due to the time for contrast material to be delivered to compartments. Aortic enhancement curve has three phases. During bolus injection phase, initial circulating contrast material inflow is performed by intravenous injection and in spite of outflow of contrast medium from this compartment the replenishment is much more dominant.

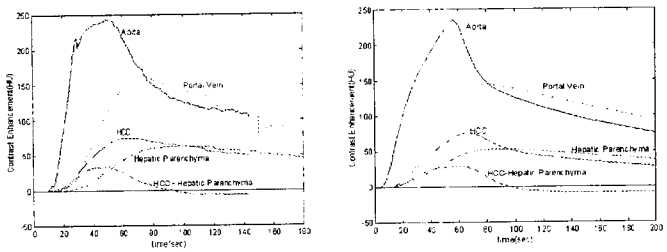

Fig. 4. (a) Averaged enhancement curves obtained from 24 patients. The determined single anatomic level was scanned dynamically after injecting 150 mg of contrast material, corresponding to an iodine load of 45 g at the rate of 3 ml/sec. Attenuation values for the tumor, hepatic parenchyma, aorta, and portal vein were obtained, and the attenuation difference between the tumor and hepatic parenchyma was plotted to test lesion detectability. (b) The simulated enhancement curves generated from dual supply model at the same condition as the clinical enhancement

Table 1. Comparison of simulation results with patient's data

Region	Enhancement peark			Peak enhancement time(sec)			Mean enhancement		
	Patients (HU)	Simulation (HU)	Difference (%)	Patients (HU)	Simulation (HU)	Difference (%)	Patients (HU)	Simulation (HU)	Difference (%)
Aorta	244.1	235.3	3.6	51.6	54.8	6.2	141.6	134.9	4.7
Portal vein	162.9	144.7	11.1	73.3	75.1	1.8	98.4	98.4	0.1
Liver parenchyma	62.5	52.8	15.4	91.2	84.8	7.0	41.5	37.5	9.7
HCC	74.8	76.2	1.8	64.5	64.5	0	49.5	44.1	10.9
Difference curve (HCC-Liver parenchyma)	35.1	29.7	15.4	50.4	57.7	14.6	8.2	8.1	0.4

Therefore, enhancement curve increases rapidly in this period. Vascular enhancement decreases rapidly in the second phase called non-equilibrium distribution period. That occurs right after the injection period and continues to the equilibrium point.

Concentration to time curve for injected contrast material in each compartment was converted to contrast enhancement (unit of HU) to time curve which can be compared with clinical result obtained in attenuation number. We referred to[6] for calibration factor.

2. Comparison with clinical data

Indivisual enhancement curves were obtained for 24 patients (21 men and 3 women aged 35-75 years) who allowed the same anatomic level to be scanned throughout the examination and then averaged at each time point over all 24 patients. We obtained mean attenuation values for the tumor, hepatic parenchyma, aorta, and portal vein. And then, the attenuation difference between the tumor and hepatic parenchyma was plotted to find the region of best conspicuity. The simulated enhancement curves generated from the model were in a good agreement with the mean enhancement curves observed in patients [fig 3 (a), (b)]. The simulated and empiric enhancements have maximum values respectively 235.3 HU, and 244.1 HU in aorta, and 76.2HU, 74.8 HU in HCC. The mean difference in maximum enhancement was 4.7% for the aortic curve and 9.7% for the hepatic curve. Several simulated values were compared with patient's data and percent differences were calculated in Table 1.

3. Effects of Injection Protocols on lesion detection

Though previous studies have demonstrated that detection of hepatic lesions with computed tomography is improved by enhancement of the liver with contrast material administered intravenously, the most advantageous method for administering intravenous contrast material for enhancement of the liver at CT is not clear. We simulated the contrast enhancement at CT for various conditions with the model mentioned above, and observed how the lesion detectability varies according to the injection protocol. We defined two kinds of parameter, Tw and Ad, for hepatic lesion detectability. Tw (temporal window) is the time interval in which the contrast enhancement difference between

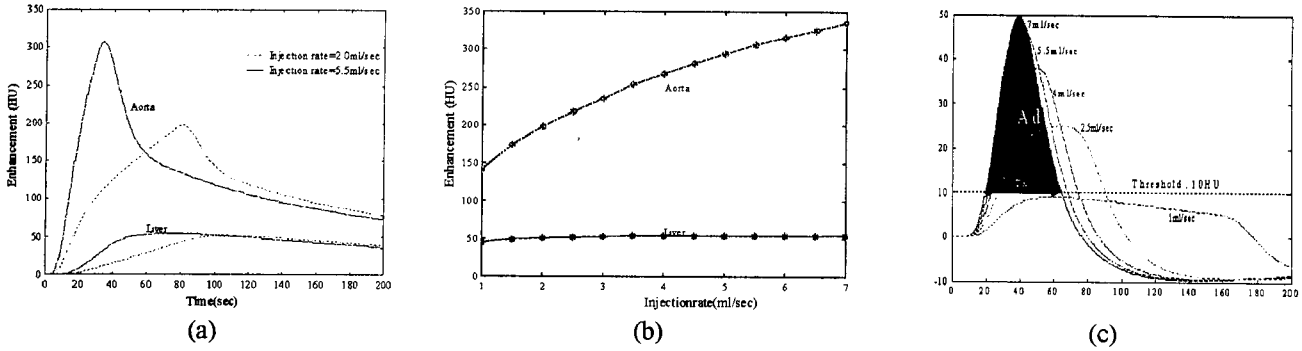

Fig. 5. (a) Enhancement curves for two different injection rates. The volume and concentration of injected contrast medium were fixed to 150 ml and 300 mg/ml, respectively. (b) Relationship between injection rate and peak enhancement. (c) The difference of enhancement between HCC compartment and hepatic parenchyma

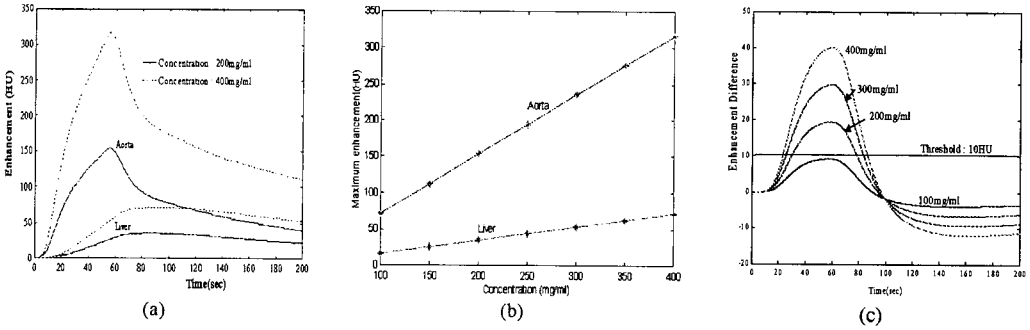

Fig. 6. (a) Enhancement curves for two different contrast medium concentration. The volume and injection rate were fixed to 150 ml and 3 ml/sec, respectively. (b) Relationship between concentration and peak enhancement. (c) Enhancement difference between HCC compartment and hepatic parenchyma

HCC and liver parenchyma exceeds defined threshold. In this study, desirable tumor enhancement was defined as tumor enhancement of 10 HU above or below the liver enhancement. Ad (area of detection region) is the area under the enhancement curve segment exceeding threshold. In figure 5 (c), the shaded area represents the Ad at 7ml/sec of injection rate with 150 ml injection volume and 300 mg/ml of contrast medium concentration.

(1) Effects of Injection Rate

We simulated the effects of injection rate of contrast medium. The volume and concentration of injected contrast medium were fixed to 150 ml and 300 mg/ml, respectively. Figure 5 (a) shows the enhancement curves simultaneously for two different injection rates. When contrast medium injected at high injection rate, the injection duration was shortened and aortic peak enhancement appears more rapidly than low rate injection. There was a time delay for the curves to start enhancement in all cases. This is the bolus delivery time from the injection site to each compartment. The magnitude of peak enhancement increased with injection rate. This relationship between injection rate and peak enhancement is plotted in figure 5 (b). As shown, aortic peak enhancement increased more rapidly than hepatic peak enhancement. Aortic peak enhancement increased 136 % (from 141.9 to 335.3) with an increase in injection rate from 0.5 to 4.0 ml/sec, Hepatic peak enhancement increased 22 %(from 44.5 to 54.43) on the other hand. In figure 5 (c), we simulated the difference of enhancement between HCC compartment and hepatic parenchyma to have a grasp of injection rate effect on lesion detectability. The shaded area represents the Ad at 7 ml/sec of injection rate. This parameter was defined as the area under the enhancement difference curve above a desired level (threshold 10 HU). Though temporal window (Tw) decreases as injection rate increases, the mean enhancement value increases more rapidly, therefore Ad value increases finally (Table 2). That is to say, if we use high injection rates, we can get clear lesion detection at the expense of long detectable time.

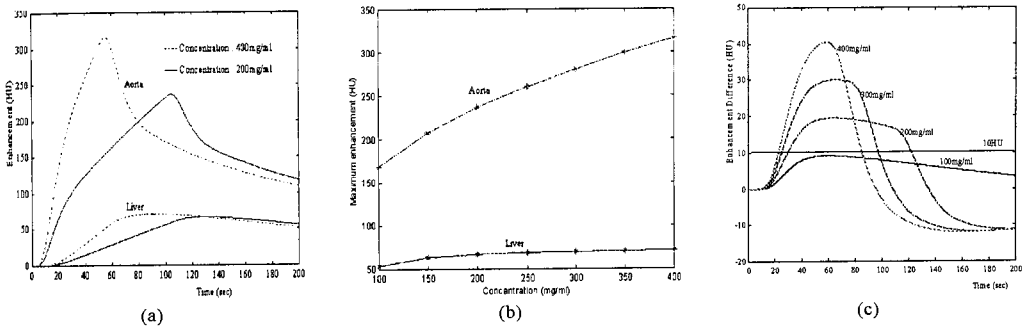

(a) (b) (c)

Fig. 7. (a) Enhancement cures for two different contrast medium concentration. The injection rate and total amount of mass of injected contrast medium were fixed to 3 ml/sec and 450 g, respectively. (b) Relationship between concentration and peak enhancement. (c) Enhancement difference between HCC compartment and hepatic parenchyma

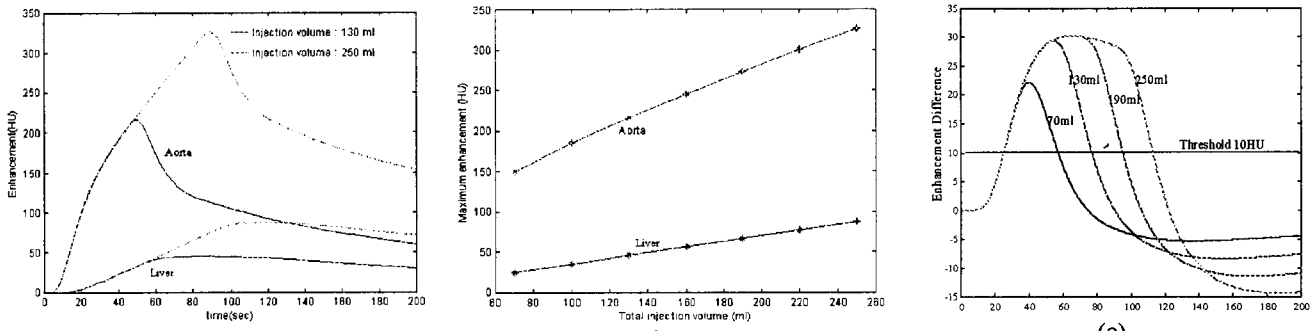

(a) (b) (c)

Fig. 8. (a) Enhancement curves for two different injection volumes simulation at the fixed injection rate (3 ml/sec) and fixed concentration (300 mg/ml). (b) Relationship between injection volume and peak enhancement. (c) Enhancement difference between HCC compartment and hepatic parenchyma

Table 2. Injection rate effects on lesion detectability

Injection rate (ml/sec)	Twindow (sec)	Enhancement difference mean value(HU)	Area (HU x sec)
1.0	0	0	0
1.5	83.4	3.2	263.1
2.0	70.9	7.4	524.6
2.5	63.5	10.6	672.7
3.0	58.5	13.0	764.9
3.5	53.4	15.6	833.8
4.0	51.1	17.1	874.3
4.5	49.7	18.2	905.2
5.0	48.3	19.1	927.2

Table 3. Concentration effects on lesion detectability (fixed volume and injection rate)

Concentration (mg/ml)	Twindow (sec)	Enhancement difference mean value(HU)	Area (HU x sec)
100	0	0	0
150	38.2	3.0	115.2
200	47.9	6.5	314.2
250	53.9	9.9	524.2
300	57.6	13.2	764.4
350	60.8	16.4	1000.9
400	64.1	19.3	1241.2

(2) Effects of Contrast medium Concentration

Concentration effects of injected material were analyzed by two processes. In the first process, we fixed injection volume(ml) and injection rate[figure 6]. Therefore, concentration (mg/ml) variation causes the variation of total amount of injection mass (mg). In this case the parameters showed linear increase as the concentration increases. In the second process, we fixed total amount of injection mass and varied concentration. So, increased concentration means decreased injection volume. This causes the same results as the case of increased injection rate at fixed volume and concentration [figure 7]. Therefore, even though total amount of injection mass is same, the lesion detectability can be elevated at the low volume and high concentration. It is more effective to use high concentration and low dose

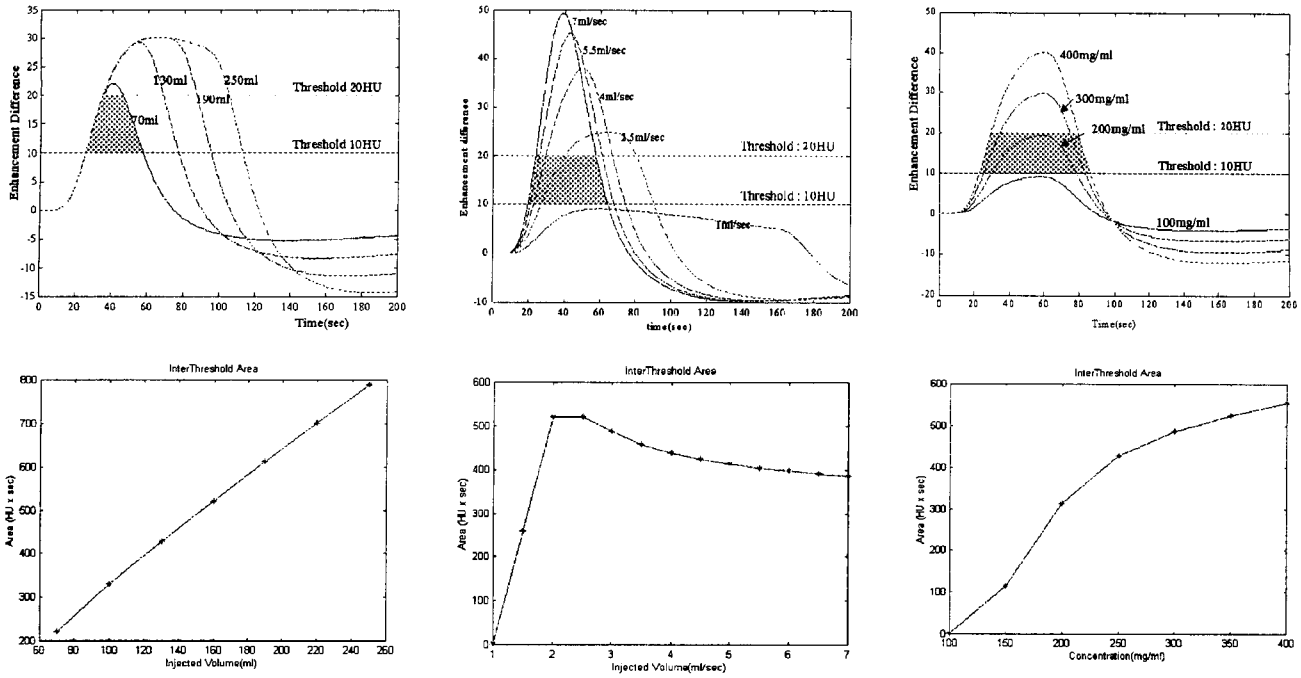

Fig. 9. In the graphs above, we assumed that the threshold of desirable contrast is 10 HU and the threshold of overmuch or luxurious contrast is 20 HU. The area integral of a given contrast curve between 10 and 20 HU represents both the length of temporal window and the optimal contrast. Plotting those area integral values provided graphs below. Left column: effect of the volume of contrast material, center: effect of injection rate, right column: effect of contrast material concentration

Table 4. Concentration effects on lesion detectability (fixed mass and injection rate)

Concentration (mg/ml)	Twindow (sec)	Enhancement difference mean value(HU)	Area (HU x sec)
100	0	0	0
150	101.8	3.0	280.8
200	92.2	7.0	678.0
250	79.3	11.0	912.7
300	71.4	15.0	1057.0
350	65.9	18.0	1161.5
400	62.2	20.0	1230.7

at the same injection mass, or to use fast injection rate at the same dose. On the other hand, if the contrast material is injected during the same time, the mass injection rate (mg/sec) determines the enhancement pattern. That is, though the injection volume rate is low, the concentration can fill up the deficiency of total volume.

(3) Effects of Injection Volume

The effects of injection volume were assessed by simulation at the fixed injection rate (3 ml/sec) and fixed concentration (300 mg/ml). As shown in figure 8 and table 5, all kinds of parameters (Tw, Ad, enhancement peak, mean enhancement difference) increased linearly as injection volume increased, which meets our expectations. Therefore we can surmise from these results that the more injection volume give rise to the better lesion detectability. But it must remain in the limit of safety.

Table 5. Injected volume effects on lesion detectability

Concentration (mg/ml)	Twindow (sec)	Enhancement difference mean value(HU)	Area (HU x sec)
100	0	0	0
150	101.8	3.0	280.8
200	92.2	7.0	678.0
250	79.3	11.0	912.7
300	71.4	15.0	1057.0
350	65.9	18.0	1161.5
400	62.2	20.0	1230.7

CONCLUSION

The delivery of contrast material to the liver after peripheral intravenous injection is influenced by numerous factors. In this study, we developed a physiological model of contrast medium enhancement containing HCC compartment.

Blood supply to liver was modeled in two paths. The first path is by hepatic artery and the second is by portal vein. It is assumed that only hepatic artery can supply blood to hepatocellular carcinoma (HCC) compartment. To test the utility of this model, we compared simulation results with clinical data obtained from 24 patients at the same condition. And then analyzed the effects of various injection protocols on hepatic lesion detectability. These may help to optimize the scanning protocols for good diagnosis. For this purpose, we considered the conspicuity as the parameter to decide lesion detectability. It is defined as the area between two thresholds in the lesion-to-liver contrast curve. The upper threshold was set to 20HU, and we regard it luxurious or overmuch if the contrast difference exceeds this value. The lower threshold was 10HU that was considered as the minimum contrast difference to distinguish lesion from normal tissue. Figure 9 shows the conspicuities in various injection protocols. This study may help to optimize scanning protocols for better diagnosis. Furthermore, a simple modification of our pharmacokinetic model allows the simulation of various pathologic models such as focal lesions other than HCC, cirrhosis, obstruction of hepatic vein, and transient hepatic attenuation difference of various causes such as arterioportal shunt.

REFERENCES

1. Baron RL, "*Understanding and optimizing use of contrast material for CT of the liver*", Am J Roentgenol, Vol. 163, pp.323-331, 1994
2. Werner Krause, "*Application of Pharmacokinetics to computed tomography*", Investigative Radiology, Vol. 31, pp. 91-100, 1996
3. T. Irie, S.Suzuki, T. Yamauchi and S. Kusano, "*Predition of the time to peak hepatic enhancement to optimize contrast-enhanced spiral CT*", Acta radiologica, Vol. 36, pp. 154-158, 1995
4. Ian H.Cox, W. Dennis Foley, Raymond G. Hoffmann, "*Right window for dynamic hepatic CT*", Radiology, Vol. 181, pp. 18-19, 1991
5. Marilyn M. Walkey, "*Dynamic hepatic CT : How many years will it take 'Till we learn?*", Radiology, Vol. 181, pp. 17-18, 1991
6. Kyongtae T. Bae, Jay P. Heiken, James A. Brink, "*Aortic and hepatic peak enhancement at CT: Part I. Pedition with computermodel*", Radiology, Vol. 207, pp. 647-655, 1998
7. Minor WR. "*Cardiovascular physiology*", Oxford. England: Oxford University press,1990
8. Vincent C. Rideout. "*Mathematical and Computer Modeling of Physiological system. Prictice-Hall*", pp. 27:65, 1991
9. Kyongtae T. Bae, Jay P. Heiken, James A. Brink, "*Aortic and hepatic peak enhancement at CT: Effect of contrast medium injection rate-pharmacokinetic analysis and experimental porcine model*", Radiology, Vol. 206, pp. 455-464,1998